Talanta 117 (2013) 39–44

Contents lists available at ScienceDirect

Talanta

journal homepage: www.elsevier.com/locate/talanta

# The time-resolved D-SERS vibrational spectra of pesticide thiram

Pan Li [a], Honglin Liu [b], Liangbao Yang [b,*], Jinhuai Liu [b,*]

[a] Department of Chemistry, University of Science & Technology of China, Hefei, Anhui 230026, China
[b] Institute of Intelligent Machines, Chinese Academy of Sciences, Hefei 230031, China

ARTICLE INFO

*Article history:*
Received 27 May 2013
Received in revised form
19 August 2013
Accepted 28 August 2013
Available online 3 September 2013

*Keywords:*
Time-resolved
Au nanoparticle
Surface enhanced Raman spectroscopy
Thiram
Fingerprints information

ABSTRACT

Time-resolved dynamic-SERS (D-SERS) can observe the process of chemical reaction between target and substrate and changes of adsorptive forms for analytes. In this paper, the vibrational spectra of pesticide thiram adsorbed on Au nanoparticles and intensity alternation of SERS spectra depended on different laser powers have been systematically investigated using the method of D-SERS. The Raman intensities of $b_2$ and $a_1$ modes of thiram related to the standard band appear different regulars with the extending time. Meanwhile, due to SERS vibrational spectra of pesticide thiram at different concentrations exhibit different SERS signals, the results of time-resolve D-SERS demonstrate the breakdown of band and different adsorptive forms of molecule on Au substrate. The continuous time-resolved the spectroscopic method offers the fingerprints of target molecules and provides great practical potentials for the continuous assessment and identification of pesticide or other probe molecules.



## 1. Introduction

The structure and binding features of molecules in nano-junctions or nanoparticles surface are critically important for understanding the function and performance of nano-science. To observe the chemical reaction or adsorption between molecules and metal nanoparticles, various methods such as spectroscopic [1–2] and microscopic ones [3–4] have been developed. However, most of these methods require sophisticated instruments, complex sampling processes or lack sufficient recognition capability for different molecules and cannot obtain original signals from the samples, which limits their wider application. Among the various techniques that have been applied in practical areas, SERS is one of the most favorable methods for obtaining the structural information of the target molecules [5–7]. Due to advantages of providing vibrational spectroscopic fingerprints and acquiring nondestructive signals, SERS has been widely used in many fields. Recently, much more strong driving forces promote SERS technique to nontraditional but important surface analysis, which is required in material science [8–10], environmental pollutants/biological monitor and inspection [11–12], and the public/food safety with determination of surface molecules at living cells/organisms [13–14], the probe of dynamite particulates [15–16] and the detection of pesticides [17–19] residues in agricultural products. On the other hand, it is well known that the large signal enhancement in SERS originates from the nature of nano-aggregates, particularly on the interparticle distance. With regard to this issue, Li et al. [20] have proposed a method by fabricating flexible gold nanorod arrays that can form hot spots in solution for detection and identification of probe molecule.

In our previous study, we also have proposed the metastable state surface-enhanced Raman scattering called D-SERS [21–23]. In this method, nanoparticle suspension with target molecules acting as D-SERS substrate was dropped onto Si wafer without using any surfactant or capping reagent. During the volatilization process, the nanoparticles keep moving to form self-assembly state until the liquids have disappeared, at the same time, continuous time-resolve SERS spectra can be calculated. Because of calculating continuous time-resolve spectra, the fine change for target molecule or the chemical reaction between analyte and Au (Ag) nanoparticles would be observed. Moreover, the driving force for self-assembly into clusters is short-range attraction coming from the solvent capillary forces, which effectively acts as surface tension leading to a decrease in surface energy upon aggregation. Additionally, the balance between short-range attraction and long-range Coulomb repulsion provides a stabilizing mechanism against gelation and determines a finite aggregation number. Furthermore, two classical types of mechanisms, electromagnetic field enhancement (EM) and chemical enhancement (CT) are also suitable for interpreting D-SERS. Importantly, through this time-resolved D-SERS method for detection of molecules, we can observe the fingerprints of molecules or chemical process of molecule interacted with substrate.

Thiram has been widely used as a protective fungicide on field crops, vegetables, and fruits. The biological activity of thiram is based on the chemical properties of the dithio-carbamate group, which can react with HS-containing enzymes and coenzymes of fungal cells, thus blocking their catalytic activity [24]. Although

* Corresponding authors. Tel.: +86 551 5592385; fax: +86 551 5592420.
*E-mail addresses:* lbyang@iim.ac.cn (L. Yang), jhliu@iim.ac.cn (J. Liu).

0039-9140/$ - see front matter © 2013 Elsevier B.V. All rights reserved.
http://dx.doi.org/10.1016/j.talanta.2013.08.050

acute toxicity of thiram is a little low, it can also be irritants to skin and mucous membranes, and upon chronic exposure it is suspected carcinogens and teratogen [17]. Consequently, it should be of great interest to develop a sensitive method to analyze and detect this small molecule in soils, water and foods, as well as the chemical state at which it is retained in these systems.

On the basis of the above reports about the toxicity of thiram and advantages of the time-resolved D-SERS method, we carried out a systematic study of thiram adsorbed on Au nanoparticles. The detailed discussions concerning the effect of different laser power to time-resolved D-SERS spectra of thiram and adsorptive structure of this organic compound upon $10^{-5}$ M and $10^{-6}$ M concentrations are afforded. In this work, using the method of time-resolved D-SERS for detection of target molecules with continuous spectra, the fingerprints of molecules or changes of adsorptive forms have been obtained.

## 2. Experimental

### 2.1. Reagents

Trisodium citrate, chloroauric acid ($HAuCl_4$) was purchased from Sinopharm Chemical Reagent Co., Ltd. (Shanghai, China). All the chemicals used were of analytical grade or better and were used without further purification.

### 2.2. Apparatus

Fourier-transform IR (FT-IR) spectra were obtained using a Nicolet-8700 spectrophotometer. Raman spectra were carried out on a LabRAM HR800 con-focal microscope Raman system (Horiba Jobin Yvon). The time-resolved Raman spectra were immediately recorded with 633 nm laser with 10 mW power and 50× objectives (1.5 μm$^2$ spot). The integral time is 2 s, and the slit aperture is 100 μm. The interval period for the collection of the Raman spectra was set at 2.5 s.

### 2.3. Preparation of FTIR sample

The FTIR of solid was described with the transmittance and the FTIR of solution was described with absorption or transmittance, however, both of two descriptions or measurements could indicated the functional groups of molecules. The solid sample was mixed with the KBr solid, then, mixture were pestled, tabletted and examined with FTIR measurements. This FTIR was the transmittance measurements. The liquid sample was dropped into the KBr solid, then, mixtures were stoved, pestled and tabletted, finally examined with FTIR measurements, and this FTIR was the absorption or transmittance measurements.

## 3. Results and discussion

The method of time-resolved D-SERS was based on the strategy that is nanoparticles could self-close to form “hot spot” driven by the solvent volatilizing [23]. The whole volatilization process took place less than 10 min, meanwhile, the solvent would also protect the target molecules and SERS substrate from laser damage, consequently, the achievement of the continuous time-resolved SERS spectra would reflect the real and fingerprint vibrational spectra of target molecules. On the other hand, the SERS intensity is increasing during the solvent volatilizing process. Fig. 1 showed the time-resolved SERS intensity alternation of Raman peaks of thiram ($10^{-5}$ M) with the different attenuations of Laser power. For the convenience of comparison, all the Raman spectra have been represented using the Raman intensities of the 1375 cm$^{-1}$ and 1505 cm$^{-1}$ peaks as standard. As shown in

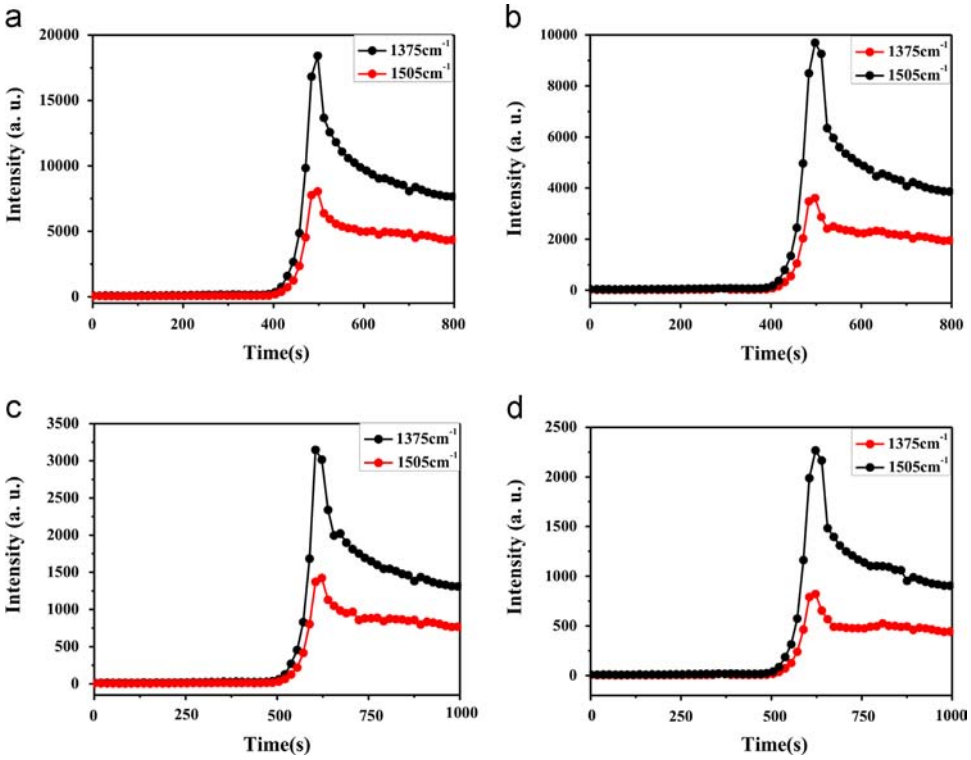


**Fig. 1.** SERS intensity alternation of time-resolved Raman peaks at 1375 cm$^{-1}$ and 1505 cm$^{-1}$ of thiram ($10^{-5}$ M) with the different attenuation of laser powers (a) D0.6-10 mW, (b) D1-5 mW, (c) D2–1 mW (d) D3-0.5 mW at the interval of 2.5 s, dropping the mixture of 0.5 μL thiram and 0.5 μL Au NPs substrate on the glass slide. All time-resolved Raman spectra were recorded with a 633 laser and 2 s acquisition time.

Fig. 1, with the increasing of the laser power decay, the time-resolved relative Raman intensities of two bands decreased steadily. It is well known that laser power plays an important role in getting SERS intensities with the traditional SERS analytical method [25]. On the basis of above data, the laser power also had an impact on the continuous time-resolved D-SERS intensities, which was well consistent with the traditional fact. Moreover, with the volatilization process intensifying, the time-resolved Raman intensities of bands steadily increased and then decreased, finally kept equilibrium after the highest signal spot. During the process of steadily increasing and keeping equilibrium, much more information about vibrational spectra and adsorptive structure of target molecules could be easily observed.

Since a similar laser power dependent behavior was observed for the four different laser powers investigated above, laser power 5 mw (D0.6) was selected for a better discussion due to the strong SERS signal and good signal-to-noise ratio. Fig. 2a showed the time-resolved SERS spectra of thiram ($10^{-5}$ M). The main Raman bands included 556 $cm^{-1}$ assigned to υ(S–S) band, 924 $cm^{-1}$ to υ(C–S) band, 1144 $cm^{-1}$ to ρ(HCN)+($CH_3$), 1375 $cm^{-1}$ to $\delta_s(CH_3)$ coupled with υ(C–N), 1505 $cm^{-1}$ to $\delta_{as}(CH_3)$ coupled with υ(C–N), respectively. Also, the shoulder band 1438 $cm^{-1}$ could be not observed carefully. However, the SERS spectra above mentioned were different from the normal Raman of thiram powder [18,24]. As shown in Fig. 2a, the band at 556 $cm^{-1}$ υ(S–S) was greatly decreased and bands at 849 $cm^{-1}$ and 1040 $cm^{-1}$ in comparison to the normal Raman of thiram powder were disappeared. On the other hand, the band at 1505 $cm^{-1}$ to $\delta_{as}(CH_3)$ coupled with υ(C–N) was strongly enhanced in comparison to the normal Raman. These results are in accord with the literature [24] and imply that S−S bond of thiram molecule is easily broken due to possible catalysis effect of metal NPs, which gave rise to radical structures that were strongly adsorbed onto Au NPs.

In addition, interestingly, with the extending of time, the relative Raman intensity of $b_2$ and $a_1$ mode appeared different results. Also, for the convenience of comparison, the Raman intensity of the band at 1375 $cm^{-1}$ was used as standard. Besides this convenience, compared with other band, the Raman peak 1375 $cm^{-1}$ is stable in different concentrations without shifting and vanished. Fig. 2b carefully showed the relative Raman intensity of $b_2$ mode υ(S–S) to standard band increased drastically from 0.11 to 0.13, 0.15 and 0.17. In contrast, the relative Raman intensity of $a_1$ mode $\delta_{as}(CH_3)$ to standard band decreased drastically from 0.65 to 0.45, 0.45 and 0.35. It should be noted that during the process of collecting continuous time-resolved Raman spectra, charge transfer (CT) [26–27] mechanism also made many contributions to the Raman signals, though the enhanced orders of magnitude were less than the electromagnetic mechanism (EM) [28]. On the basis of this result, the collecting of continuous time-resolved Raman spectra was beneficial to observe the changing of molecules structure because of contribution of chemical mechanism, obtaining the fingerprint vibrational spectra and adsorptive radical structure.

The SERS spectra of thiram underwent important changes upon varying the concentration. Fig. 3a showed the time-resolved D-SERS spectra of thiram ($10^{-6}$ M). Decreasing the thiram concentration, some changes were observed: the SERS spectra of $10^{-6}$ mol/L thiram with relating to that of $10^{-5}$ mol/L thiram a new band at 1565 $cm^{-1}$ was appeared which was ascribed to the formation of υ(C=N) [29], furthermore, the shoulder band could be clearly observed and emerged blue-shift from 1438 $cm^{-1}$ to 1408 $cm^{-1}$. On the other hand, Fig. 3b exhibited the blue-shift and broadening of band 1565 $cm^{-1}$ and Fig. 3c and d proved that 1565 $cm^{-1}$ was a new band that was appearing later 34 s than the known bands 1375 $cm^{-1}$ or 1505 $cm^{-1}$ with the increasing of time. The blue-shift and broadening of band at 1565 $cm^{-1}$ and intensity increasing of $b_2$ modes can be well explained with the CT mechanism during the process of collecting time-resolved D-SERS spectra. This result further proved that vibrational spectra, representing molecular fingerprint

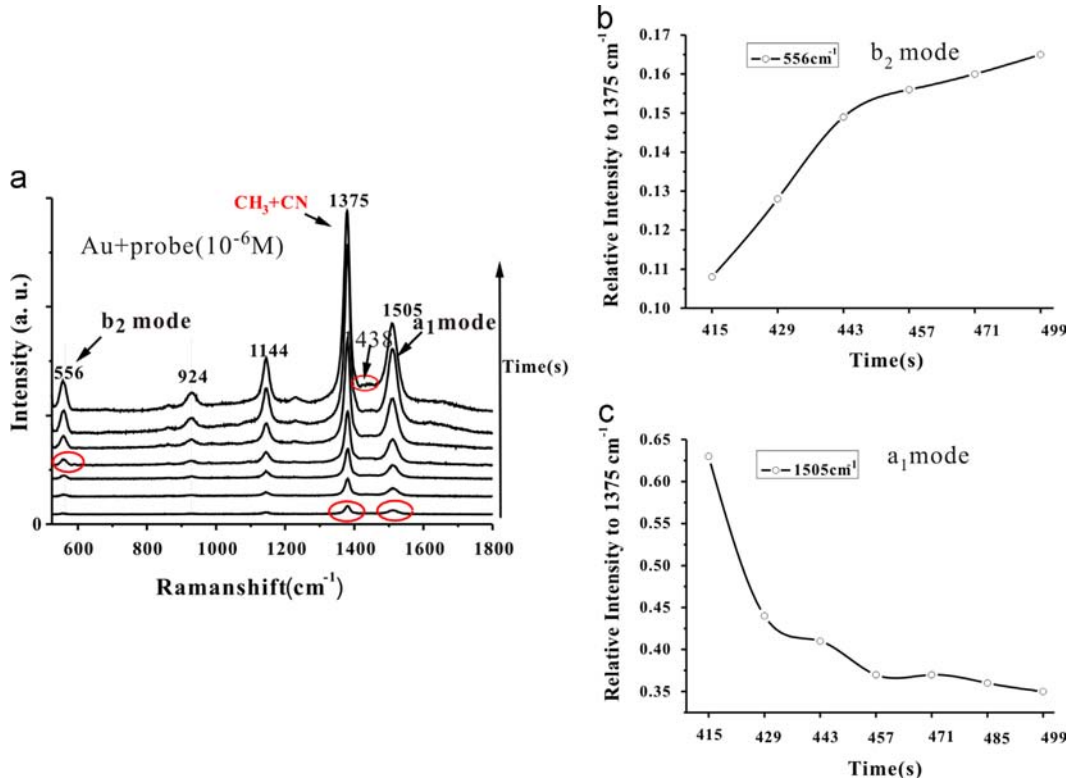


**Fig. 2.** (a) SERS spectra of time-resolved of thiram ($10^{-5}$M) and time-dependent relative Raman intensity of bands (b) at 556 $cm^{-1}$ and (c) at 1505 $cm^{-1}$ to at 1375 $cm^{-1}$. All time-resolved Raman spectra were recorded with a 633 nm laser, 2 s acquisition time and at interval of 2.5 s. Laser power was 10 mW.

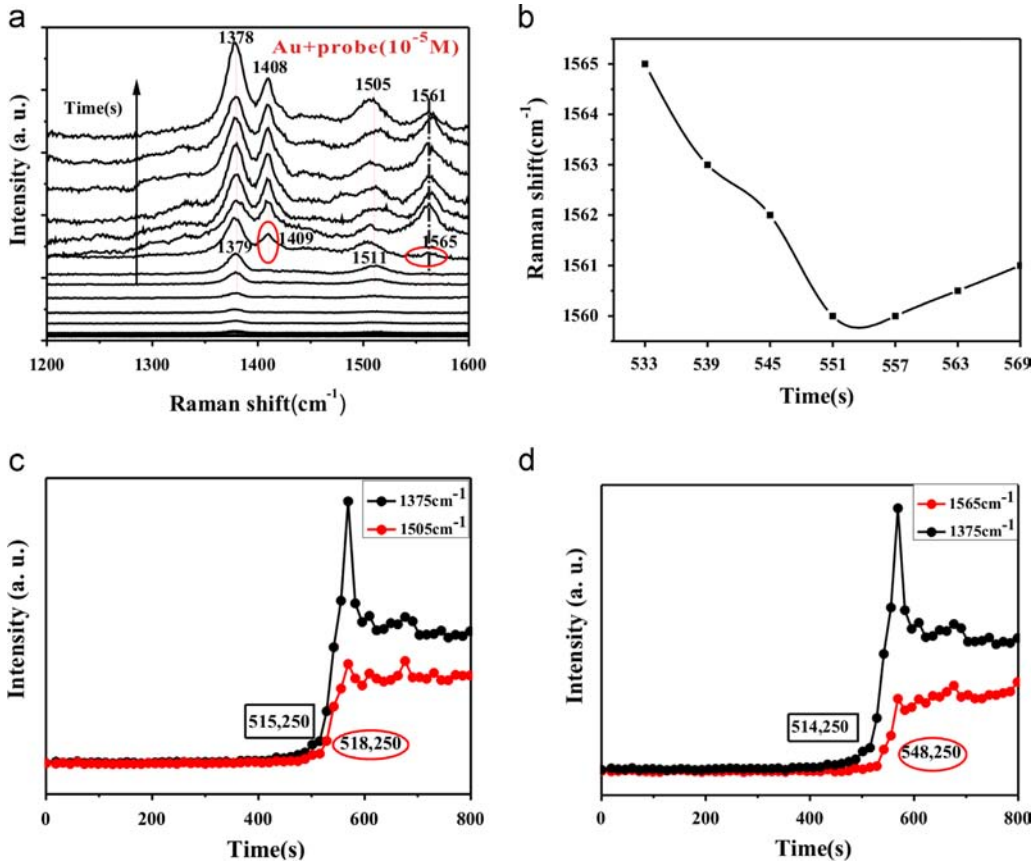


**Fig. 3.** (a) SERS spectra of time-resolved of thiram ($10^{-6}$ M) and (b) alternation of time-depend of band at 1565 $cm^{-1}$. SERS spectra relative alternation of time-resolved Raman peaks (c) at 1505 $cm^{-1}$ and (d) at 1565 $cm^{-1}$ to standard band at 1375 $cm^{-1}$. All time-resolved Raman spectra were recorded with a 633 nm laser and laser power was 10 mW.

characteristics, can be obtained from the low concentration of pesticide though the continuous time-resolved D-SERS method.

Moreover, it is well known that the position of υ(C=N) around 1560 $cm^{-1}$, which induced the attraction of the free electron pair in the N atom and the creation of the υ(C=N) bond, could be used for estimating the interaction strength of this ligand with Au NPs [30]. At the $10^{-6}$ M concentration, the band 1565 $cm^{-1}$ underwent blue-shifting and broadening, indicating the increasing of υ(C=N) character and strong interaction with Au NPs. Meantime, the υ(C=N) band appearing at 1565 $cm^{-1}$ should be assigned to bi-thio groups interacted with Au NPs. Because under such orientation and form, the υ(C=N) vibration was perpendicular to Au NPs, thus contributing to the enhancement of the 1565 $cm^{-1}$ band. In addition, the predominant signal of mono-thiol adsorptive form possibly also lead to disappearance or decreased of bi-thiol adsorptive structure signal at $10^{-5}$ M concentration. The observed band at 1408 $cm^{-1}$ was possibly attributed to forming of new adsorptive structure. Comparing Fig. 2a, this band 1408 $cm^{-1}$ in Fig. 3a appeared strong signals and position shifting with respect to the band at 1375 $cm^{-1}$ when the concentration of pesticide was modified. As a consequence, it should be noted that the observation of 1408 $cm^{-1}$ proved the emerging of new adsorptive structure [31]. On the basis of above results, we deduced that thiram was adsorbed on the Au NPs though two different coordination structures: (i) bi-thiol adsorbed on the Au NPs, forming C=N structure and (ii) mono-thiol adsorbed on the Au NPs, forming the C–N structure. These two different bands have been also observed in the monomer solid state [32].

The difference of time-resolved SERS spectra between $10^{-5}$ M and $10^{-6}$ M concentrations could be explained by these two different adsorptive structures. At $10^{-5}$ M concentration, the mono-thiol adsorptive structures predominates, however, at $10^{-6}$ M concentration, the bi-thiol adsorptive form and mono-thiol adsorptive form existed simultaneously, because of the appearing and blue-shift of new band at 1565 $cm^{-1}$ and the strong signal of shoulder band at 1408 $cm^{-1}$. Meanwhile, two bands 1565 $cm^{-1}$ and 1408 $cm^{-1}$ in $10^{-5}$ M contributions indicated the important role of chemical mechanism in observing the time-resolved D-SERS spectra.

As shown in Fig. 4a, different SERS spectra have been exhibited with different concentrations. At the $10^{-5}$ M concentration, the mono-thiol adsorptive structures predominated, due to the vibrational spectra of band υ(C=N) have not been observed. At the $10^{-6}$ M concentration, both of vibrational band υ(C–N) at 1505 $cm^{-1}$ and band υ(C=N) at 1565 $cm^{-1}$ have been monitored, therefore, the bi-thiol adsorptive form and mono-thiol adsorptive form existed simultaneously. The existing of two adsorptive structures at $10^{-6}$ M concentration was probably due to the higher surface of two thiols adsorptive form available for the absorption on the Au NPs. On the other hand, the FTIR experiment has been observed, which was also consistent with above results. The FTIR spectra of different thiram concentrations with Au NPs were shown in Fig. 4b. The band 1090 $cm^{-1}$ was assigned to vibration υ(C–N), the band 1629 $cm^{-1}$ to vibration υ(C=N). As exhibited in Fig. 4b, the vibration υ(C–N) predominated in the $10^{-5}$ M concentration which was the mono-thiol adsorptive form, and the vibration υ(C–N) and υ(C=N) both have been obtained in the $10^{-6}$ M concentration, which indicated the two adsorptive forms emerged simultaneously. This conclusion was well consistent with that of the time-resolved D-SERS spectra of thiram. Moreover, the changes of υ(C=S) [33] was also

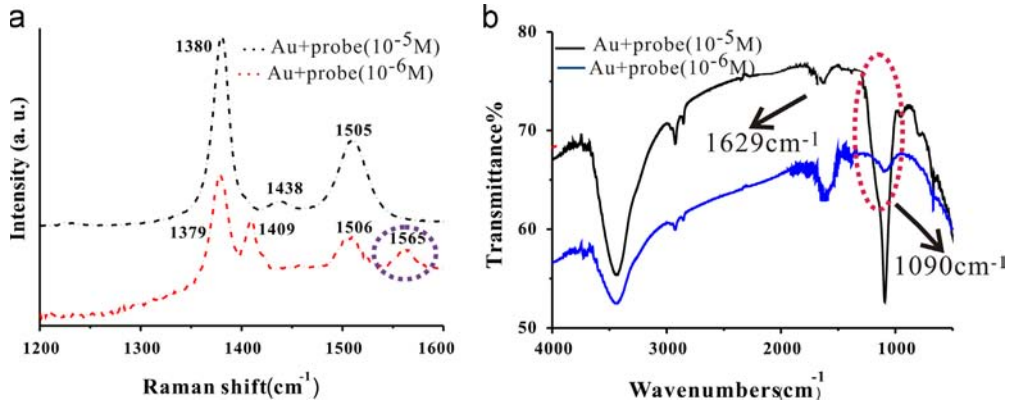


**Fig. 4.** (a) The comparison of SERS and (b) FTIR spectra of different thiram concentrations with Au NPs.

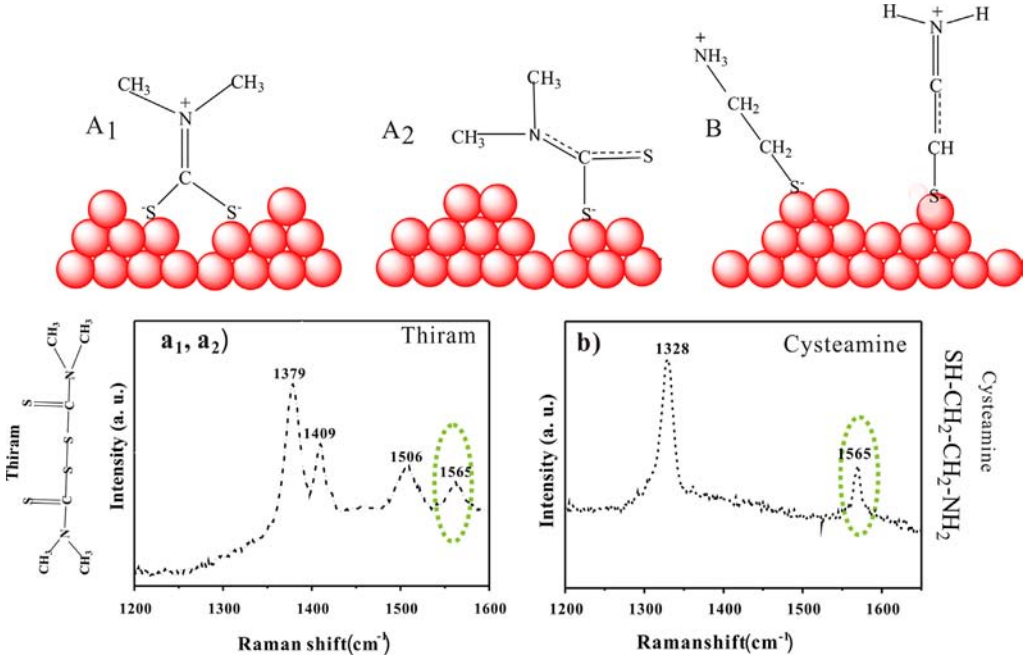


**Fig. 5.** Possible adsorptive mechanisms, and SERS spectra of thiram and cysteamine respectively. All the Raman spectra were recorded with a 633 nm laser and laser power was 10 mW.

interpreted this characteristics, which was expected to appear in the 900–1000 $cm^{-1}$ region. However, this band was much more difficult to observe due to weak SERS signal.

Interestingly, there was also difference between the solid Raman and SERS spectra of Cysteamine. As shown in Fig. S1, the band at 1510 $cm^{-1}$ assigned to υ(C–N) has been enhanced and appeared large red-shift to 1565 $cm^{-1}$ attributed to υ(C=N), which proved the molecular adsorptive structure was changed on the Au NPs. In other words, the adsorptive form of cysteamine on the Au NPs was agreed with the υ(C=N) structure of thiram with the bi-thiol groups, perpendicular to Au NPs. Thus, collecting the time-resolved D-SERS spectra of typical molecules was beneficial to analyze and deduce the possible adsorptive forms of traditional probe molecules and functional SERS molecules, such as cysteamine, cysteine.

On the basis of above characteristics, the results suggested that the thiram underwent a breakdown in the S−S bond to the formation of two different adsorptive fragments due to the possible catalysis effect of Au metal NPs. As shown in Fig. 5$a_1$, 5$A_2$, thiram was adsorbed on the Au NPs with two structures: mono-thiol adsorptive form with the band υ(C–N); bi-thiol adsorptive form with the band υ(C=N). The new band 1565 $cm^{-1}$ of cysteamine was obtained to show the possible alternation of adsorptive form in Fig. 5b.

## 4. Conclusions

The continuous spectra of time-resolved D-SERS of thiram studies were carried out at several laser powers. On the other hand, different adsorptive concentrations were revealed the thiram can interact with Au NPs through two coordination forms: mono-thiol and bi-thiol adsorbed on Au NPs. Moreover, different probe concentrations appeared different spectra. At $10^{-5}$ M concentration, the mono-thiol adsorptive structures predominates, while at $10^{-6}$ M concentration, the bi-thiol adsorptive form and mono-thiol adsorptive form existed simultaneously: the bi-thiol adsorptive structure was monitored at 1565 $cm^{-1}$ with υ(C=N); mono-thiol form was also observed at 1505 $cm^{-1}$ with υ(C–N). In addition, the time-resolved D-SERS spectra further could be employed for the analytical detection of this pesticide and also

beneficial to study the chemical state in environment by these characteristics. Also, we can deduce the degradation process of environmental pollutant and improved the understanding of potential environmental impact through the continuous time-resolved D-SERS spectra. Nevertheless, further experiments would be needed to evaluate the forming of two adsorptive structures.

## Acknowledgments

This work was supported by the National Basic Research Program of China (2011CB933700), the National Instrumentation Program of China (2011YQ0301241001 and 2011YQ0301241101), the Important Projects of Anhui Provincial Education Department (KJ2010ZD09).

## References

[1] X.L. Wang, C.M. Lieber, J. Am. Chem. Soc. 110 (1988) 5200–5201.
[2] P.C. Lang, D. Meisel, J. Phys. Chem. 86 (1982) 3391–3395.
[3] K.W. Brett, C. Dean, J. Campbell, B.R. Herr, C.A. Mirkin, J. Am. Chem. Soc. 117 (1995) 6071–6082.
[4] P.E. Laibinis, G.M. Whitesides, J. Am. Chem. Soc. 114 (1992) 9022–9028.
[5] H.P. Zhang, Y.F. Huang, G.K. Liu, D.Y. Wu, B. Ren, Z.Q. Tian, J. Am. Chem. Soc. 132 (2010) 9244–9246.
[6] S.M. Jensen, J. Am. Chem. Soc. 131 (2009) 4090–4098.
[7] C.C. Maria, R.L. Birke, J.R. Lombardi, J. Phys. Chem. C 112 (2008) 20295–20300.
[8] X. Ling, L. Xie, Y. Fang, H. Xu, H. Zhang, J. Kong, M.S. Dresselhaus, J.Z. Liu, Nano Lett. 10 (2010) 553–561.
[9] E.J. Quinn, A.H. Santana, D.M. Hutson, C.M. Pegrum, D. Graham, W.E. Smith, Small 3 (2007) 1394–1397.
[10] N.P. Rajesh, V. Kannan, M. Ashok, K. Sivaji, P.S. Raghavan, P. Ramasamy, J. Cryst. Growth 262 (2004) 561–566.
[11] J.H. Lee, K.S. Jeon, D.K. Lim, H. Kim, S.H. Kwon, H.M. Lee, Y.D. Suh, ACS Nano 6 (2012) 9574–9584.
[12] D. Li, J.S. Fossey, Y.T. Long, Anal. Chem. 82 (2010) 9299–9305.
[13] J. Li, L. Chen, T. Lou, Y. Wang, Appl. Mater. Interfaces 3 (2011) 3936–3941.
[14] D. Li, L. Qu, W. Zhai, J. Xue, J.S. Fossey, Y.T. Long, Environ. Sci. Technol. 45 (2011) 4046–4052.
[15] M. Lopez, J.L. Ferrando, C.G. Ruiz, Anal. Chem. 85 (2013) 2595–2600.
[16] H.B. Zhou, Z.P. Zhang, C.L. Jiang, G.J. Guan, K. Zhang, Q.S. Mei, R.Y. Liu, S.H. Wang, Anal. Chem. 83 (2011) 6913–6917.
[17] B. Saute, R. Premasiri, L. Ziegler, R. Narayanan, Analyst 137 (2012) 5082–5087.
[18] B.H. Liu, G.J. Gan, Z.P. Zhang, R.Y. Liu, C.L. Jiang, S.H. Wang, M.Y. Han, Anal. Chem. 84 (2012) 255–261.
[19] J.C. Costa, R.A. Ando, A.C. Santana, L.M. Rossi, P.S. Santos, M.L. Temperini, P. Corio, Phys. Chem. Chem. Phys. 11 (2009) 7491–7498.
[20] F.S. Hu, W. Wu, I. Naumov, X.M. Li, A.M. Bratkovsky, Z.L. Stanley Williams, J. Am. Chem. Soc. 132 (2010) 12820–12822.
[21] K. Qian, L.B. Yang, Z.Y. Li, J.H. Liu, J. Raman Spectrosc. 44 (2013) 21–28.
[22] L.B. Yang, H.L. Liu, Y.M. Ma, J.H. Liu, Analyst 137 (2012) 1547–1549.
[23] L.B. Yang, H.L. Liu, J. Wang, F. Zhou, Z.Q. Tian, J.H. Liu, Chem. Commun. 47 (2011) 3583–3587.
[24] C.D Sanchez-Cortes, J.V. Garcı´a-Ramos, J.A. Azna´ rez, Langmuir 17 (2001) 1157–1162.
[25] G.K Liu, P.C. Zheng, G.L. Shen, J.H. Jiang, R.Q. Yu, Y. Cui, B. Ren, J. Phys. Chem. C 112 (2008) 6499–6508.
[26] L.B. Yang, W.D. Ruan, J.X. Yang, B. Zhao, W.Q. Xu, J.R. Lombardi, J. Phys. Chem. C 113 (2009) 16226–16231.
[27] G.F. Celly, M.S. Izumi, L.A. Temperini, J. Phys. Chem. B 112 (2008) 16334–16340.
[28] T.J. Norman, C.D. Grant, A.M. Schwartzberg, J.Z. Zhang, Opt. Mater. 27 (2005) 1197–1203.
[29] A. Frigerio, B. Halac, M. Perec, Inorg. Chim. Acta. 164 (1989) 149–154.
[30] P. Dumas, N. Spassky, P. Sigwalt, J. Polym., Sci. Pol. Chem. 12 (1974) 1001–1010.
[31] M.V. Sanchez-Cortes, O. Francioso, J.V. Ramos, Vib. Spectrosc. 17 (1998) 133–144.
[32] D.A. Brown, W.K. Glass, M.A. Burke, Spectrochim. Acta 32A (1976) 137–139.
[33] F. Bonati, R.J. Ugo, Org. Chem. 10 (1967) 257–259.